AGU PUBLICATIONS

Geophysical Research Letters

RESEARCH LETTER
10.1002/2014GL062921

Key Points:
- Mantle geochemical variability and heterogeneity
- Preservation of He isotope signatures in mantle-derived melts

Correspondence to:
B. Mougel,
mougel@ipgp.fr

Citation:
Mougel, B., M. Moreira, and A. Agranier (2015), A "high $^4He/^3He$" mantle material detected under the East Pacific Rise (15°4′N), *Geophys. Res. Lett.*, *42*, 1375–1383, doi:10.1002/2014GL062921.

Received 18 DEC 2014
Accepted 6 FEB 2015
Accepted article online 10 FEB 2015
Published online 13 MAR 2015

A "high $^4He/^3He$" mantle material detected under the East Pacific Rise (15°4′N)

Berengere Mougel[1,2], Manuel Moreira[1], and Arnaud Agranier[2]

[1]Institut de Physique du Globe de Paris, Sorbonne Paris Cité CNRS, UMR, Paris, France, [2]Laboratoire Domaines Océaniques, UMR6538, IUEM, Plouzane, France

Abstract We investigate in details helium isotope data reported in Mougel et al. (2014) for 14 basaltic samples collected on the East Pacific Rise by submersible (15°4′N) where the ridge interacts with the Mathematician seamounts. Samples locations are separated by only few hundred meters across a 15 km along-axis profile. The data reveal a strong geochemical variability that has never been observed at such high spatial resolution for helium isotope compositions. Moreover, they reveal an unusually high $^4He/^3He$ mantle component also characterized by unradiogenic lead, atypical in oceanic basalts. He-Pb systematics suggests a mixture between a nonradiogenic lead and radiogenic helium pyroxenitic component, recycled from the deep continental lithosphere and the ambient peridotitic mantle. The He isotope difference between these two end-members can be interpreted as a time evolution of two distinct mantle sources after a slight $(U+Th)/^3He$ fractionation, likely due to some ancient degassing during the formation of deep continental pyroxenites.

1. Introduction

Helium (He) isotopes, coupled with heavy radiogenic isotopes, have been utilized for decades in order to explore the nature, structure, and evolution of the Earth's mantle. While ^4He comes mostly from the radioactive decay of uranium (^{235}U, ^{238}U) and thorium (^{232}Th), ^3He is considered primordial. The preferred materials for analyzing He isotopes are the quenched glassy rims of pillow lavas, as well as melt and fluid inclusions in minerals because they are less sensitive to degassing. Global compilation of the He isotopic data in oceanic basalts has revealed that most ocean island basalts (OIB) have low and variable $^4He/^3He$ ratios (or high *R*/*Ra* where *R* is the $^3He/^4He$ ratio normalized to air), whereas most mid-ocean ridge basalts (MORB) have higher and more homogeneous $^4He/^3He$ ratios with a mean value of $90{,}000 \pm 10{,}000$ ($R/Ra = 8 \pm 1$) [*Allègre et al.,* 1995]. MORB and OIB are therefore interpreted as sampling two different mantle reservoirs. OIB sample a more primitive (enriched in ^3He) deep mantle reservoir, while MORB tap the degassed upper mantle [*Kurz et al.,* 1982; *Allègre et al.,* 1983; *Kaneoka*, 1983]. Nevertheless, higher than MORB $^4He/^3He$ (e.g., $>120{,}000$; $R/Ra < 6$) are also reported in oceanic basalts. Such samples can be found on St. Helena, Tristan da Cunha, Sao Miguel Islands, or in HIMU-Type OIB [e.g., *Moreira et al.,* 1999*; Graham et al.,* 1993*; Moreira et al.,* 2012*; Hanyu and Kaneoka,* 1997*; Class et al.,* 2005*; Barfod et al.,* 1999], but this peculiar radiogenic helium signature is not common in MORB, especially when posteruptive radiogenic production is excluded. These "high $^4He/^3He$ hot spots" reflect either the presence of recycled materials [*Hanyu and Kaneoka*, 1997] or isotopic perturbations induced by late and shallow processes [*Hilton et al.,* 1999]. The coupling of He isotopes with other isotopic tracers, therefore, provides insight into the origin and nature of radiogenic He materials in the mantle. Furthermore, studying He isotope variability at various spatial scales in erupted lavas along oceanic spreading centers is also fundamental in order to understand the length scale(s) of mantle heterogeneities and the preservation of their signature at the surface. Despite apparent He isotopes homogeneity in worldwide MORB from the entire ridge system, some local variations between single ridge segments exist [*Georgen et al.,* 2003]. These may reflect the presence of mantle heterogeneities (e.g., petrological anomalies such as fertile recycled veined material or small mantle plumes) propagating through the upper mantle and melting beneath or close to ridges.

This paper represents one of the highest spatial resolutions for He isotopic studies attempted on a single ridge segment. Fourteen basaltic samples were collected during submersible dives around 15°4′N along the East Pacific Rise (EPR) (Figure 1) where the Mathematician hot spot track intercepts the ridge and were analyzed for their He and lead (Pb) isotope compositions. Our results show an atypical straight correlation between these two isotope systems suggesting the mixture of two distinct mantle components. They also

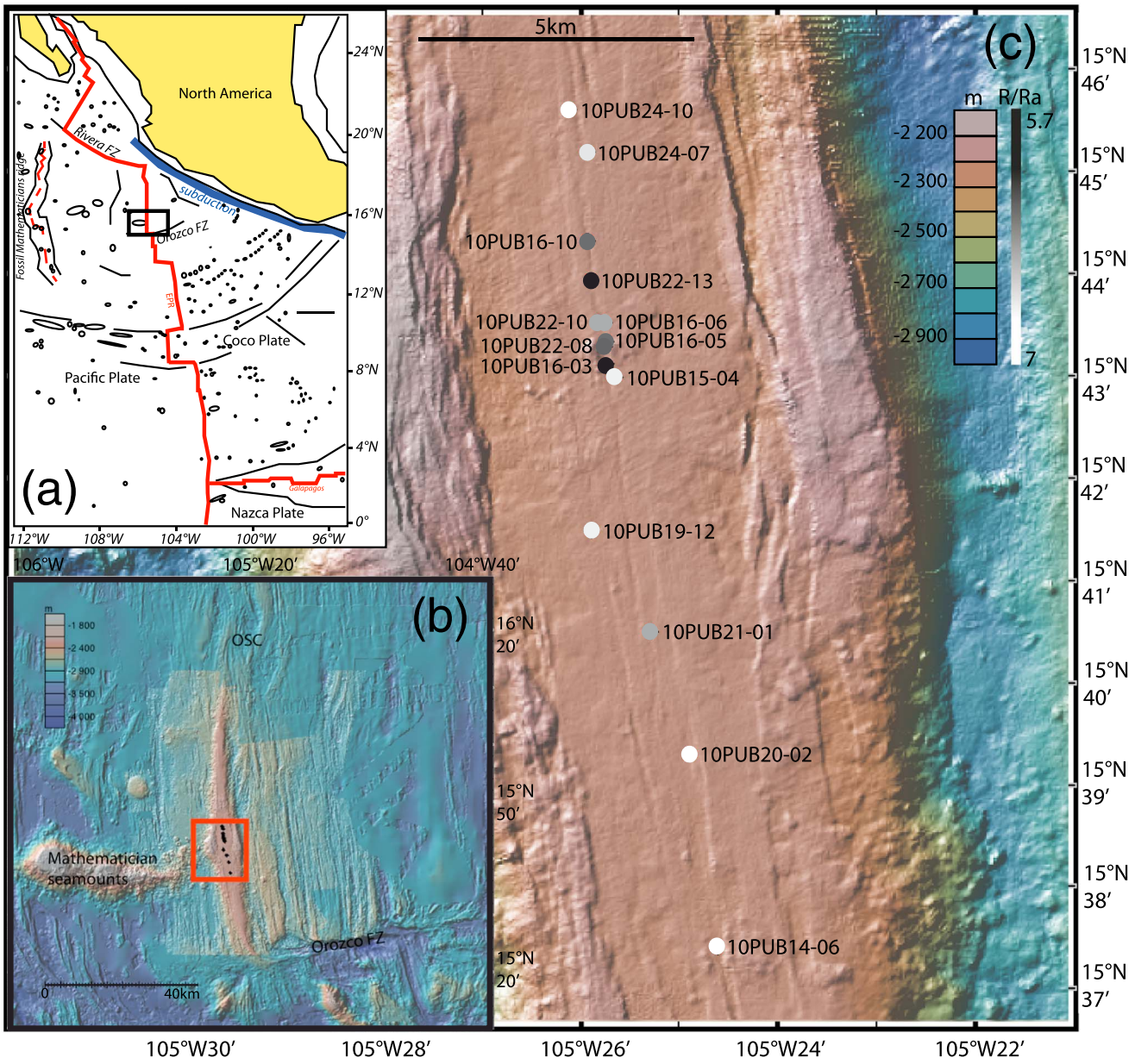

Figure 1. Sample locations and bathymetric maps of the study area. (a) Simplified global map showing the location of the study area (black square). (b) Main physiographic features and localization of the study (red rectangle). (c) Zoom on the study area (40 m grid spacing) showing the sample locations and their helium isotopic compositions and distribution along the EPR axis between 15°37′N and 15°46′N. The color of the symbols represents the helium isotope composition from the most radiogenic in black ($R/Ra = 5.7$) to the least radiogenic in white ($R/Ra = 7$).

suggest the existence of a radiogenic He mantle heterogeneity beneath this area already marked by a highly unradiogenic Pb composition. The strong isotopic variability in this spatially restricted area is another important and unexpected characteristic of this 20 km^2 zone along a ridge segment. In this study, we investigate the origin of this "high ^{4}He/^{3}He" mantle source and its He isotopic divergence from ambient mantle value.

2. Geologic Outline of the Study Area

The northern part of the EPR separates the Pacific and Cocos plates with a full spreading rate of ~85 mm/yr [*Carbotte et al.,* 1998]. Between Rivera and Orozco Fracture zones (FZ), the ridge is offset by two discontinuities

that have divided the ridge into three segments, which have axial morphologies that are drastically different from one another. This study focuses on the southern segment (Figure 1), located on the northern side of Orozco FZ. It is 115 km long, and is 400 m shallower (-2200 m) and twice as wide (~10 km wide) as the rest of the EPR [e.g., *Scheirer and Macdonald*, 1993; *Weiland and Macdonald*, 1996; *Carbotte et al.,* 2000]. The ridge axis is intercepted perpendicularly on its western side by a prominent seamount chain named "P1545" [*Macdonald et al.,* 1992; *Weiland and Macdonald*, 1996; *Carlut et al.,* 2004]. Previous studies attributed this singular morphology to a remarkably high magmatic supply due to the presence of a hot spot [e.g., *Scheirer and Macdonald*, 1995; *Weiland and Macdonald*, 1996; *Carbotte et al.,* 2000; *Shah and Buck*, 2006; *Le Saout et al.,* 2014] named "Mathematician hot spot" [*Le Saout et al.,* 2014; *Mougel et al.,* 2014] which may also be responsible for the two-step western segment migration during the last 300 ka [*Carbotte et al.,* 2000]. The geochemical composition of basalts from this area is also quite notable [*Mougel et al.,* 2014] as it displays a geochemical variability that has never been observed along a ridge at such a small spatial scale (<20 km of ridge axis), including a novel mantle signature (Unradiogenic Lead Component; ULC) related to the hot spot [*Mougel et al.,* 2014]. The range of isotopic compositions of these basalts is commensurable to that of the entire EPR and can be accounted for by a mixture of three main components representative of the hot spot heterogeneity and its interaction with the ridge. The particularity of ULC-influenced basalts is a very unradiogenic Pb signature ($^{208}Pb/^{204}Pb = 36.83$, $^{207}Pb/^{204}Pb = 15.46$, and $^{206}Pb/^{204}Pb = 17.49$) associated with mostly enriched Sr, Nd, and Hf isotopic compositions ($^{87}Sr/^{86}Sr = 0.70303$, $^{143}Nd/^{144}Nd = 0.51303$, and $^{176}Hf/^{177}Hf = 0.28302$), which is different from any known mantle end-members. An ancient (>2 Ga) lower continental origin for this material has been formerly proposed [*Mougel et al.,* 2014], with the involvement of sulfides invoked in order to explain the unradiogenic Pb compositions. The current preferred model suggested by trace element and isotope compositions is the recycling and sequestration within the upper mantle of sulfide-bearing pyroxenites coming from a continental arc root [*Mougel et al.,* 2014]. Finally, the melting of the heterogeneous hot spot source and its connection with the ridge system then enables rapid and abundant melt transfer toward the ridge [*Mittelstaedt et al.,* 2011], preserving the signatures of the heterogeneities in the MORB despite efficient mixing.

3. Samples and Methods

Samples of basaltic glass were collected "in situ" with the French submersible Nautile during the PARISUB cruise (R/V *L'Atalante* March–April 2010) along the EPR axis, between 15°37′N and 15°46′N [*Gente et al.,* 2010]. The combination of high precision bathymetric data (Autonomous Underwater Vehicle acquisitions) and the use of the submersible allowed very accurate positioning of each sample. Volcanic glass chips were handpicked under a microscope and ultrasonically cleaned in ultra pure water and ethanol. Sample locations are given in Figure 1.

For He data acquisition, glass fragments (≤4 mm) were melted under vacuum and gas was extracted, purified, and transferred to the mass spectrometer using the automated line connected to the Noblesse© mass spectrometer at Institut de Physique du Globe de Paris (IPGP). The ^{4}He blank was $\sim 2 \times 10^{-10}$ ccSTP (Cubic Centimeter Standard Temperature Pressure) during the course of the measurements. The detailed procedure on Noblesse is given in *Moreira et al.* [2011]. Pb isotope data were obtained from HF-HNO_3 dissolution of ~500 mg of sample (after HCl leaching) following the protocol described in *Blichert-Toft et al.* [2005] and *Agranier et al.* [2005]. Isotopic compositions were analyzed using the Thermo Neptune Multiple Collector-Inductively Coupled Plasma-Mass Spectrometer (MC-ICP-MS) of Ifremer Brest. Values used for mass bias fractionation corrections are $^{205}Tl/^{203}Tl = 2.388$. Those used for standard bracketing are those from *Todt et al.* [1996]. These isotopic data have been previously reported in the supporting information of a former paper [*Mougel et al.,* 2014]. We now add the He concentrations of the samples.

4. Results

He and Pb data are given in Table 1. The $^{4}He/^{3}He$ ratios vary from 103,818 to 126,762 (*R/Ra* between 5.70 and 6.96). These data represent much more radiogenic compositions than "regular" MORB value (~90,000; *R/Ra* ~8) [*Allègre et al.,* 1995; *Graham*, 2002] and are therefore not typical of a major hot spot signature such as Hawaii [*Kurz et al.,* 1983, 1987], Iceland [*Graham et al.,* 1998; *Hilton et al.,* 1999], or Galapagos [*Kurz et al.,* 2009], which show low $^{4}He/^{3}He$ (high *R/Ra*) ratios compared to MORB (down to 15,000) [*Stuart et al.,* 2003]. He concentrations in our samples are also typical of MORB ranging from 1.0×10^{-5} to 1.9×10^{-5} ccSTP/g.

Table 1. Helium and Lead Isotopic Compositions of the Studied Samples[a]

Sample	Longitude	Latitude	Weight(g)	^{4}He(ccSTP/g)	^{4}He/^{3}He	2σ	*R/Ra*	2σ	^{206}Pb/^{204}Pb	^{207}Pb/^{204}Pb	^{208}Pb/^{204}Pb
10PUB16-05	−105.429	15.722	0.021	1.2×10^{-5}	120,424	2008	6.00	0.10	17.494	15.461	36.831
10PUB22-10	−105.430	15.725	0.034	1.9×10^{-5}	112,196	2090	6.44	0.12	17.930	15.473	37.282
10PUB22-13	−105.431	15.732	0.022	1.2×10^{-5}	126,762	2224	5.70	0.10	17.507	15.459	36.835
10PUB16-10	−105.432	15.739	0.031	1.4×10^{-5}	120,424	2008	6.00	0.10	17.608	15.464	36.950
10PUB16-03	−105.429	15.719	0.025	1.5×10^{-5}	125,008	2162	5.78	0.10	17.619	15.459	36.946
10PUB16-06	−105.429	15.725	0.029	1.4×10^{-5}	112,196	1742	6.44	0.10	17.820	15.473	37.173
10PUB22-08	−105.429	15.722	0.027	1.2×10^{-5}	123,091	2096	5.87	0.10	17.498	15.467	36.831
10PUB21-01	−105.421	15.675	0.027	1.1×10^{-5}	112,916	2090	6.44	0.12	17.831	15.488	37.117
10PUB20-02	−105.415	15.655	0.033	1.5×10^{-5}	106,256	1876	6.80	0.12	18.171	15.497	37.558
10PUB15-04	−105.427	15.716	0.029	1.5×10^{-5}	105,790	1858	6.83	0.12	18.149	15.494	37.522
10PUB14-06	−105.410	15.623	0.025	1.5×10^{-5}	103,841	1790	6.96	0.12	18.180	15.491	37.538
10PUB24-07	−105.432	15.753	0.027	1.0×10^{-5}	106,727	1892	6.77	0.12	18.199	15.506	37.593
10PUB24-10	−105.435	15.760	0.036	1.6×10^{-5}	103,963	2094	6.95	0.14	18.163	15.500	37.553
10PUB19-12	−105.432	15.691	0.029	1.1×10^{-5}	104,716	1822	6.90	0.12	18.191	15.506	37.583

[a] *Ra* is the ^{3}He/^{4}He atmospheric ratio ($=1.384\times10^{-6}$).

Figure 1 illustrates the spatial distribution of He isotopic signatures in samples. The most radiogenic compositions are concentrated within a 2 km very restricted area around 15°44′, precisely where the ridge axis and the seamounts seems to connect. Pb isotopes feature low ratios for oceanic basalts: ^{206}Pb/^{204}Pb = 17.49–18.20, ^{207}Pb/^{204}Pb = 15.46–15.51, and ^{208}Pb/^{204}Pb = 36.83–37.59. Both He and Pb isotopes also show wide range of compositions for such a restricted area (<20 km^2). Plotted together, they define a clear correlation illustrated in Figure 2. In this figure, samples depict an atypical trend where ^{4}He/^{3}He decreases (R/Ra increases) as the ^{206}Pb/^{204}Pb ratios increase; it is the opposite direction for the rest of Pacific and Atlantic data where radiogenic helium are associated to radiogenic lead. Only DUPAL-like Indian basalts appear to have a similar global correlation; however, they involve less radiogenic He compositions (Figure 2). On the contrary, the most radiogenic He signatures found for Atlantic and Pacific basalts correspond the most radiogenic Pb signatures, which follows logically given that Pb isotopes and ^{4}He are both daughter products of the same radiogenic parents, and that recycling of oceanic crust in the mantle implies both high U/Pb and U/^{3}He ratios.

5. Discussion

Low ^{4}He/^{3}He ratios in OIB have been attributed to the sampling of a deep primitive mantle reservoir, while more radiogenic He compositions in MORB have been attributed to liquids that have tapped a more degassed upper mantle (e.g., higher (U + Th)/^{3}He). Here we identify a new high ^{4}He/^{3}He hot spot, sampling material from the upper part of the mantle and affecting the EPR. Since its discovery in Tristan da Cunha and Gough magmatic rocks [*Kurz et al.,* 1982], the origin of such radiogenic He signature is still debated. It has been demonstrated that degassing and radiogenic production of He in the magma chambers [*Zindler and Hart*, 1986; *Moreira and Allègre,* 2004], posteruptive alpha implantation into olivine rims [*Moreira et al.,* 2012], and crustal assimilation [*Hilton et al.,* 1995] are shallow processes that can largely impact the magmatic He isotopic composition and mask the mantle-derived signature. Therefore, high ^{4}He/^{3}He ratios have to be interpreted carefully, particularly for low He concentrations. However, all these processes should mainly disturb He isotopic compositions and induce a decoupling of He from the other isotopic tracers. In this study, data depict a statistically strong correlation ($r^2 = 0{,}94$) between He and Pb ratios, providing evidence that the samples reflect the He isotopic compositions of contributing mantle sources. Moreover, because their concentrations (10^{-5} cc/g) are not low for MORB (which could render them easily prone to crustal contamination), these results confidently provide information on their mantle source compositions and history.

A high ^{4}He/^{3}He ratio implies a high (U + Th)/^{3}He integrated ratio. Subducted material has already been considered as a radiogenic He reservoir [*Kurz et al.,* 1987] because of the degassing of the oceanic lithosphere during both its formation at mid-ocean ridge and its subduction (during metamorphic dehydration). Such degassing generates high (U + Th)/^{3}He material, which leads over time to a radiogenic He signature. The radiogenic He contents of HIMU-like oceanic islands have confirmed this hypothesis [e.g., *Hanyu and Kaneoka*,

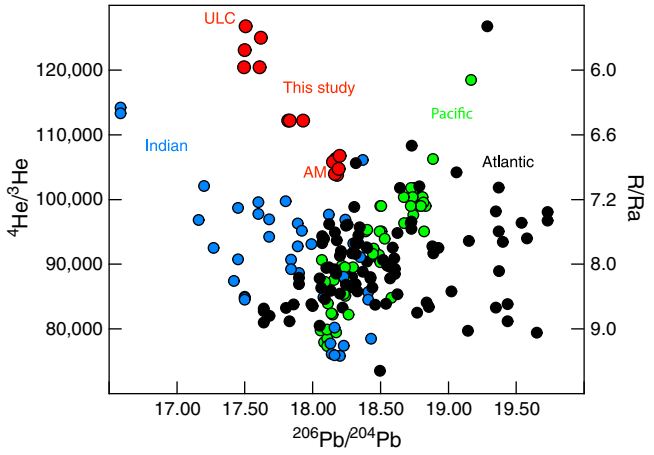

Figure 2. Binary plot representing helium isotope compositions $^{4}He/^{3}He$ versus $^{206}Pb/^{204}Pb$. Basalts from this study are represented as red circles and are compared to basalts from Atlantic (black), Pacific (green), and Indian (blue) oceanic domains [*Kurz et al.*, 1982; *Graham et al.*, 1992; *Dosso et al.*, 1993; *Mahoney et al.*, 1994; *Dosso et al.*, 1999; *Gautheron*, 2002; *Moreira and Allègre*, 2002; *Kurz et al.*, 2005; *Meyzen et al.*, 2007; *Moreira et al.*, 2008; *Hamelin et al.*, 2011]. Error bars are smaller than the size of the symbols.

1997; *Barfod et al.,* 1999; *Christensen et al.,* 2001; *Parai et al.,* 2009]. However, high $^{4}He/^{3}He$ hot spots origin appears to be much more diverse. For example, delamination of subcontinental lithosphere has also been proposed to explain the origin of other radiogenic He plumes (e.g., São Miguel of the Azores) [*Moreira et al.,* 2012]. Continental crust is known for being highly degassed [*Ballentine*, 1*997; Graham,* 2002], and He isotope ratios measured in ultramafic xenoliths from continental lithospheric mantle [*Porcelli et al.,* 1987*; Dunai and Porcelli,* 2002*; Gautheron and Moreira,* 2002] are as high as those observed for high $^{4}He/^{3}He$ oceanic basalts. Therefore, the recycling of such material into the upper mantle should also contribute to the formation of a radiogenic He mantle reservoir. However, despite many differences, based on a global compilation of trace element and isotopic data, *Class et al.* [2005] showed that high $^{4}He/^{3}He$ OIB have common characteristics that differentiate them from other MORB and more "primitive" OIB. They have the highest U + Th concentrations and the highest $^{206}Pb/^{204}Pb$ and $^{208}Pb/^{204}Pb$ ratios for a given $^{143}Nd/^{144}Nd$ ratio. Basalts from this study do not have such high U and Th concentrations, nor radiogenic Pb, but do have clearly higher $^{4}He/^{3}He$ ratios than MORB, and therefore depict an atypical high $^{4}He/^{3}He$ mantle signature. Following the model of *Lee et al.* [2012], *Mougel et al.* [2014] have proposed that this signature reflects a previously unknown mantle end-member, which may be constituted of metagabbroic and sulfide-rich pyroxenites that were delaminated from ancient continental arc root, and could be consistent with this atypical Pb-He isotopic correlation.

This correlation is in conformity with a mixture of two main components, i.e., the ambient local mantle (AM) and ULC [*Mougel et al.,* 2014]. The extremely wide range of isotopic compositions of samples at very small spatial scale along the ridge axis (Figure 1) is more likely explained by shallow along-axis mixing of melts, which would be coherent with a fast-spreading ridge system, especially one interacting with a hot spot. This diversity of He isotopic compositions at such a small spatial scale has rarely been observed in oceanic basalts, whereas He isotopic heterogeneities were easily identified at first and second orders of segmentation along ridges (from more than 300 to 50 km), especially in hot spot-ridge interaction systems. Reasons for this could be (1) the lack of geochemical studies dedicated to very small-scale area with submersible sampling approach, (2) mixing processes in the mantle and/or crust acting as an averaging mechanism, and/or (3) the rapid diffusion of He in silicates [*Hanyu and Kaneoka*, 1997; *Hart et al.,* 2008] (from 3 to 7 orders of magnitude faster than Sr, Nd, and Pb), which prevent from He isotope heterogeneities preservation on scales smaller than tens of meters, and particularly for long-term mantle in growth of ^{4}He [*Hart et al.,* 2008]. Therefore, very small veins or layers become chemically undetectable after long-term diffusion and eruptive melt processing.

One of the most glaring example of a high-resolution study recording important He isotopic variability is the 120 km^2 off-axis flow field of the EPR around 14°S, for which the $^{3}He/^{4}He$ ratio of six samples range from 8.55 to 9.22 *Ra* [*Geshi et al.,* 2007]. The mid-Atlantic ridge between 25°7′S and 26°5′S is also well documented by 14 samples that range from 7.3 to 7.7 *R/Ra* [*Graham et al.,* 1996]. Finally, *Gregg et al.* [2000] also compared two samples separated by approximately 250 m along the EPR around 9°50′N but found no differences between them. The same observation has been made for the basalts from the Lucky Strike segment in the North Atlantic where the $^{4}He/^{3}He$ ratio of 33 samples along this single ridge segment show a variation of only 1.2% (1σ) [*Moreira et al.,* 2011].

In this study, we present the He isotope compositions of 14 samples covering a single 15 km along-axis profile of an EPR segment influenced by the mathematicians hot spot, with a sampling space of 3 km to less than

50 m between 15°37′N and 15°46′N. *R*/*Ra* values range from 5.7 to 7 and therefore illustrate the preservation of moderate-amplitude He isotopic anomalies at very small spatial scale in the upper mantle. In our case, the sampling of this radiogenic He anomaly in EPR MORB is related to the presence of the Mathematician hot spot, which considerably boosts the magmatic budget of the fast-spreading ridge.

Such multi-isotopic variability and preservation are even more remarkable that they are recorded on a fast-spreading ridge system. Indeed, high degrees of partial melting would be expected to homogenize at medium and large spatial scale the mantle geochemical variability observed in MORB. However, high magmatic supply related to fast-spreading ridge system and/or a significant hot spot magma increment should, on the other hand, encourage rapid melt transfer toward the surface and incomplete mixing, which can preserved locally at small spatial scale the mantle heterogeneities. Therefore, we suggest that the most radiogenic He (i.e., ULC-influenced) basalts have sampled a component of the Mathematicians hot spot source. According to this radiogenic He signature and the limited impact of this short seamount chain on the morphology and structure of the ridge (compared to what is observed in primary, deep-rooted hot spot systems), this hot spot might be more likely a fertile upper mantle heterogeneity rather than deep mantle plume.

The size of the Mathematicians mantle heterogeneity is difficult to estimate, but according to the morphological and geochemical comparison of the study segment with the adjacent segments, it seems at most limited by the Orozco FZ (15°25′N) and the 16°20′N overlapping spreading centers (~115 km). This heterogeneity is thus likely big enough to be preserved despite long-term diffusion, whereas mesoscales He heterogeneities are rapidly homogenized with the ambient upper mantle, as suggested by the coupled diffusion-production model of *Hart et al.* [2008]. Therefore, the He isotopic difference between ULC (^{4}He/^{3}He ~ 130,000) and ambient mantle (^{4}He/^{3}He ~ 100,000) components may more likely reflect the time-integrated evolution of two separated mantle reservoirs. This difference can easily be expressed in a simple mantle evolution model that considers He degassing and radiogenic production. Pb isotopes suggest that the source of ULC is ancient, with a minimum age of 2 Ga (i.e., when the production rate of ^{207}Pb was still higher than that of the ^{206}Pb). Evolution of the number of moles of ^{4}He and ^{3}He with age τ can be described by the following equations:

$$\Delta(\tau)^3\mathrm{He} = \frac{d^3\mathrm{He}}{d\tau} = +\varphi^3\mathrm{He} \tag{1}$$

$$\Delta(\tau)^4\mathrm{He} = \frac{d^4\mathrm{He}}{d\tau} = \varphi^4\mathrm{He} - 8\lambda_8 \times {}^{238}\mathrm{U_P}\, e^{\lambda_8 t} - 7\lambda_5 \times {}^{235}\mathrm{U_P}\, e^{\lambda_5 t} - 6\lambda_2 \times {}^{232}\mathrm{Th_P}\, e^{\lambda_2 t} \tag{2}$$

Where $\Delta(\tau)^3$He represents the degassing flux of ^{3}He at mid-ocean ridge, $\lambda_8, \lambda_5, \lambda_2$, are the decay constants of ^{238}U, ^{235}U, and ^{232}Th, respectively; $^{238}U_0$, $^{235}U_0$, and $^{232}Th_0$ are the present-day concentration and φ is the degassing constant of the upper mantle (UM) ~2.2×10^{-10} yr^{-1} calculated for $^3\mathrm{He} = 10^{-10}$ cc/g in the MORB source, $\Delta(t)^3\mathrm{He} = 1000$ moles/yr, $m_{UM} = 10^{27}$ g, and $V_m^{He} = 22{,}414$ cc/mol. We also assume here that only the upper mantle is degassing. Here as τ represents age relative to present and not time, the radioactive production terms are preceded by a minus sign, and the degassing term is positive, whereas it would be the opposite if these equations were written as functions of time.

The evolution of ^{4}He/^{3}He over time (R(τ)) can therefore be written as

$$R(\tau) = R_\mathrm{P} - \frac{8\times\frac{\lambda_8}{\lambda_8-\varphi}\times{}^{238}\mathrm{U_P}\left[e^{(\lambda_8-\varphi)\tau}-1\right] + 7\times\frac{\lambda_5}{\lambda_5-\varphi}\times{}^{235}\mathrm{U_P}\left[e^{(\lambda_5-\varphi)\tau}-1\right] + 6\times\frac{\lambda_2}{\lambda_2-\varphi}\times{}^{232}\mathrm{Th_P}\left[e^{(\lambda_2-\varphi)\tau}-1\right]}{{}^3\mathrm{He_P}} \tag{3}$$

$$R(\tau) \sim R_\mathrm{P} - \left[8\times\frac{\lambda_8}{\lambda_8-\varphi}\left[e^{(\lambda_8-\varphi)\tau}-1\right] + 7\times\frac{\lambda_5}{\lambda_5-\varphi}\times\frac{1}{137.88}\left[e^{(\lambda_5-\varphi)\tau}-1\right] + 6\times\frac{\lambda_2}{\lambda_2-\varphi}\frac{\mathrm{Th}}{\mathrm{U}}\left[e^{(\lambda_2-\varphi)\tau}-1\right]\right]\left(\frac{\mathrm{U}}{{}^3\mathrm{He}}\right)_\mathrm{P} \tag{4}$$

where R_P is the present-day He isotopic ratio.

Based on *Mougel et al.* [2014] trace element data, the U content was estimated at ~12 ppb for both ULC and AM, considering 20% and 10% partial melting for pyroxenitic ULC and peridotitic AM, respectively. The mean κ ratio (Th/U) in AM-influenced samples is 3.0 and that in ULC-influenced basalts is 2.7. The

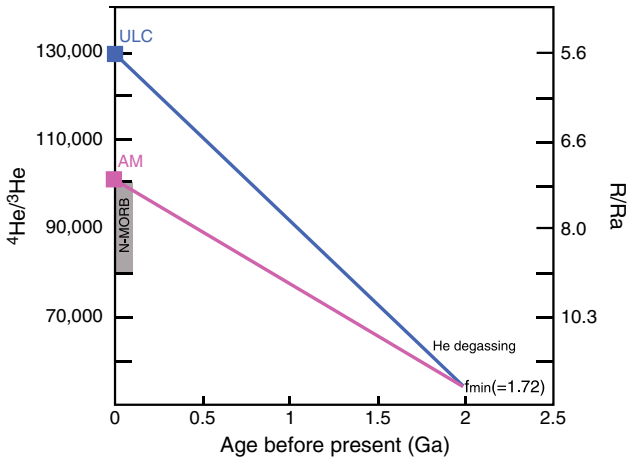

Figure 3. Helium isotopic evolution of AM (ambient local mantle) and ULC (Unradiogenic Lead Component) isolated mantle sources after a fractionation between (U + Th) and ^{3}He of ~1.72 that occurred 2 Ga ago. The model considers the same degassing constant (~2.2 10^{-10} an^{-1}) [*Moreira et al.,* 1998] for both sources. U estimated concentrations are 12 ppb for both AM and ULC. κ ratios (Th/U) are, respectively, 3 and 2.7.

results of this modeling presented in Figure 3 suggest that the most radiogenic He mantle (ULC) was likely more degassed by a factor of 1.72. Note that this is a minimum value. Indeed, as we do not have access to the true compositions of these two end-members, we approximate them by using the extreme values of the mixing line defined by our data set (For example, *f* value would increase by 0.027 by % of ULC increase). However, this hypothesis seems, therefore, compatible with the recycling of ancient lower crust material (i.e., sulfide-bearing pyroxenites) already suggested for ULC's origin by *Mougel et al.* [2014]. In agreement with this scenario, we speculate that this fractionation may have occurred during the formation of pyroxenites in the deepest part of mature continental magmatic arc [*Lee et al.,* 2012]. Since cumulates of the lower continental crust are affected by metamorphic processes during the thickening of the root, they are likely degassed during their transformation into pyroxenites, thus increasing the U/^{3}He ratio. Moreover, as Pb is chalcophile but not U, the formation and recycling of these sulfide-rich metamorphic rocks will also affect the Pb composition of ULC (U/Pb decrease). The model presented here is capable of reproducing a difference of 30,000 in the ^{4}He/^{3}He ratio of heterogeneous upper mantle material sampled by EPR. This is achieved by early (≥2 Ga) fractionation of U/^{3}He and U/Pb ratios (induced by pyroxenites formation) followed by a continuous degassing of the upper mantle and radiogenic isotope production. This model is also consistent with the negative correlation between Pb and He isotopes observed in our data.

Huang et al. [2014] have recently suggested that such cumulates would be more likely characterized by unradiogenic He. Indeed, they have proposed that He would be soluble enough in sulfide melts and trapped as inclusion in cumulates that would therefore end up enriched in He (relative to U and Th, supposed insoluble in sulfides), forming a low ^{4}He/^{3}He reservoir associated with unradiogenic Pb. Nevertheless, the negative correlation between He and Pb isotope ratios in our data indicates that such continental material could be, on contrary, radiogenic in helium, suggesting that it has a high U/^{3}He ratio. Therefore, analyzing the geochemical composition of such sulfide inclusions and continental cumulates is both valuable and necessary to understand and estimate its impact on mantle-derived melts.

6. Conclusion

Despite large melting and mixing processes induced by the high spreading rate of the ridge, MORB from along a 15 km along EPR between 15°37′N and 15°46′N reflect a particularly heterogeneous mantle domain. This segment is affected by the Mathematician seamount source, which increases the ridge's magmatic activity as well as its MORB geochemical diversity. In conjunction with Pb isotope data, He isotopes define an atypical trend for oceanic basalts. ^{4}He/^{3}He ratio correlates negatively with Pb isotope ratios, in opposition to what is observed in both the Pacific and Atlantic oceans. Furthermore, samples are characterized by radiogenic He associated with unexpectedly unradiogenic Pb that reveals the existence of an atypical high ^{4}He/^{3}He mantle heterogeneity below the EPR. The disparity in He isotopic compositions between the ambient upper mantle and this radiogenic component can be explained by a 2 Ga time-integrated evolution of the two distinct mantle reservoirs, after a slight (U + Th)/^{3}He fractionation, most likely due to the degassing of deep continental arc material.

Acknowledgments
We acknowledge the RV *L'Atalante* crew and the Nautile team for all the great work performed during the PARISUB 2010 cruise. We also thank Brandon Mahan for his careful reading of the paper. A.A. thanks the Institut National des Sciences de l'Univers and Conseil Régional de Bretagne for the financial support. Finally, Pete Burnard and Philippe Sarda are thanked for their constructive reviews. This is IPGP contribution 3607. Data supporting Figures 1 and 2 are available in Table 1.

The Editor thanks Pete Burnard and Philippe Sarda for their assistance in evaluating this paper.

References

Agranier, A., J. Blichert-Toft, D. Graham, V. Debaille, P. Schiano, and F. Albarède (2005), The spectra of isotopic heterogeneities along the mid-Atlantic Ridge, *Earth Planet. Sci. Lett.*, *238*(1–2), 96–109, doi:10.1016/j.epsl.2005.07.011.

Allègre, C. J., T. Staudacher, P. Sarda, and M. Kurz (1983), Constraints on evolution of Earth's mantle from rare gas systematics, *Nature*, *303*(5920), 762–766, doi:10.1038/303762a0.

Allègre, C. J., M. Moreira, and T. Staudacher (1995), $^{4}He/^{3}He$ dispersion and mantle convection, *Geophys. Res. Lett.*, *22*(17), 2325–2328, doi:10.1029/95GL02307.

Ballentine, C. J. (1997), Resolving the mantle He/Ne and crustal $^{21}Ne/^{22}Ne$ in well gases, *Earth Planet Sci. Lett.*, *152*, 233–249, doi:10.1016/S0012-821X(97)00142-8.

Barfod, D. N., C. J. Ballentine, A. N. Halliday, and J. G. Fitton (1999), Noble gases in the Cameroon line and the He, Ne, and Ar isotopic compositions of high μ (HIMU) mantle, *J. Geophys. Res.*, *104*(B12), 29,509–29,527, doi:10.1029/1999JB900280.

Blichert-Toft, J., A. Agranier, M. Andres, R. Kingsley, J. G. Schilling, and F. Albarede (2005), Geochemical segmentation of the Mid-Atlantic Ridge north of Iceland and ridge-hot spot interaction in the North Atlantic, *Geochem. Geophys. Geosyst.*, *6*, Q01E19, doi:10.1029/2004GC000788.

Carbotte, S., C. Mutter, J. Mutter, and G. Ponce-Correa (1998), Influence of magma supply and spreading rate on crustal magma bodies and emplacement of the extrusive layer: Insights from the east Pacific rise at lat16 degrees N, *Geology*, *26*(5), 455–458, doi:10.1130/0091-7613(1998)026<0455:IOMSAS>2.3.CO;2.

Carbotte, S. M., A. Solomon, and G. Ponce-Correa (2000), Evaluation of morphological indicators of magma supply and segmentation from a seismic reflection study of the East Pacific Rise 15°30′–17°N, *J. Geophys. Res.*, *105*(B2), 2737–2759, doi:10.1029/1999JB900245.

Carlut, J., M.-H. Cormier, D. V. Kent, K. E. Donnelly, and C. H. Langmuir (2004), Timing of volcanism along the northern East Pacific Rise based on paleointensity experiments on basaltic glasses, *J. Geophys. Res.*, *109*, B04104, doi:10.1029/2003JB002672.

Christensen, B. P., P. M. Holm, A. Jambon, and J. R. Wilson (2001), Helium, argon and lead isotopic composition of volcanics from Santo Antão and Fogo, Cape Verde Islands, *Chem. Geol.*, *178*(1–4), 127–142, doi:10.1016/S0009-2541(01)00261-3.

Class, C., S. L. Goldstein, M. Stute, M. D. Kurz, and P. Schlosser (2005), Grand Comore Island: A well-constrained "low $^{3}He/^{4}He$" mantle plume, *Earth Planet. Sci. Lett.*, *233*(3–4), 391–409, doi:10.1016/j.epsl.2005.02.029.

Dosso, L., H. Bougault, and J.-L. Joron (1993), Geochemical morphology of the North Mid-Atlantic Ridge, 10°–24°N: Trace element-isotope complementarity, *Earth Planet. Sci. Lett.*, *120*, 443–462.

Dosso, L., H. Bougault, C. Langmuir, R. C. Bollinge, R. O. Bonnie, and J. Etoubleau (1999), The age and distribution of mantle heterogeneity along the Mid-Atlantic Ridge (31–41°N), *Earth Planet. Sci. Lett.*, *170*, 269–286.

Dunai, T. J., and D. Porcelli (2002), Storage and transport of noble gases in the subcontinental lithosphere, *Rev. Mineral. Geochem.*, *47*(1), 371–409, doi:10.2138/rmg.2002.47.10.

Gautheron, C. (2002), Le manteau lithospherique sous continental contraint par la systematique des gaz rares: Apport a la geodynamique chimique des reservoirs terrestres, Thesis Univ. Paris VII, p. 252.

Gautheron, C., and M. Moreira (2002), Helium signature of the subcontinental mantle, *Earth Planet. Sci. Lett.*, *199*, 39–47.

Gente, P., et al. (2010), Cruise PARISUB on EPR 16 N magmatism and hydrothermalism over a ridge-hotspot interaction, *InterRidge News*, *19*, 17–20.

Georgen, J. E., M. D. Kurz, H. J. Dick, and J. Lin (2003), Low $^{3}He/^{4}He$ ratios in basalt glasses from the western Southwest Indian Ridge (10°–24°E), *Earth Planet. Sci. Lett.*, *206*(3–4), 509–528, doi:10.1016/S0012-821X(02)01106-8.

Geshi, N., S. Umino, H. Kumagai, J. M. Sinton, S. M. White, K. Kisimoto, and T. W. Hilde (2007), Discrete plumbing systems and heterogeneous magma sources of a 24 km3 off-axis lava field on the western flank of East Pacific Rise, 14°S, *Earth Planet. Sci. Lett.*, *258*(1–2), 61–72, doi:10.1016/j.epsl.2007.03.019.

Graham, D. W. (2002), Noble gases in geochemistry and cosmochemistry, in *Reviews in Mineralogy and Geochemistry*, edited by D. Porcelli, R. Wieler, and C. Ballentine, pp. 247–318, Miner. Soc. of Am., Washington, D. C.

Graham, D. W., W. J. Jenkins, J. G. Schilling, G. Thompson, M. D. Kurz, and S. Humphris (1992), Helium isotope geochemistry of mid-ocean ridge basalts from the South Atlantic, *Earth Planet. Sci. Lett.*, *110*, 133–147.

Graham, D. W., P. R. Castillo, J. E. Lupton, and R. Batiza (1996), Correlated He and Sr isotope ratios in South Atlantic near-ridge seamounts and implications for mantle dynamics, *Earth Planet. Sci. Lett.*, *144*(3–4), 491–503, doi:10.1016/S0012-821X(96)00172-0.

Graham, D. W., L. M. Larsen, B. B. Hanan, M. Storey, A. K. Pedersen, and J. E. Lupton (1998), Helium isotope composition of the early Iceland mantle plume inferred from the Tertiary picrites of West Greenland, *Earth Planet. Sci. Lett.*, *160*(3–4), 241–255, doi:10.1016/S0012-821X(98)00083-1.

Graham, D. W., S. E. Humphris, W. J. Jenkins, and M. D. Kurz (1993), Helium isotope geochemistry of some volcanic rocks from Saint Helena, *Earth Planet. Sci. Lett.*, *110*, 121–131.

Gregg, T. K., D. J. Fornari, M. R. Perfit, W. I. Ridley, and M. D. Kurz (2000), Using submarine lava pillars to record mid-ocean ridge eruption dynamics, *Earth Planet. Sci. Lett.*, *178*(3–4), 195–214, doi:10.1016/S0012-821X(00)00085-6.

Hamelin, C., L. Dosso, B. Hanan, M. Moreira, A. P. Kositsky, and M. Y. Thomas (2011), Geochemical portray of the Pacific Ridge: New isotopic data and statistical techniques, *Earth Planet. Sci. Lett.*, *302*, 154–162.

Hanyu, T., and I. Kaneoka (1997), The uniform and low $^{3}He/^{4}He$ ratios of HIMU basalts as evidence for their origin as recycled materials, *Nature*, *390*(6657), 273–276, doi:10.1038/36835.

Hart, S. R., M. D. Kurz, and Z. Wang (2008), Scale length of mantle heterogeneities: Constraints from helium diffusion, *Earth Planet. Sci. Lett.*, *269*(3–4), 508–517, doi:10.1016/j.epsl.2008.03.010.

Hilton, D. R., J. Barling, and G. E. Wheller (1995), Effect of shallow-level contamination on the helium isotope systematics of ocean-island lavas, *Nature*, *373*(6512), 330–333, doi:10.1038/373330a0.

Hilton, D. R., K. Grönvold, C. G. Macpherson, and P. R. Castillo (1999), Extreme $^{3}He/^{4}He$ ratios in northwest Iceland: Constraining the common component in mantle plumes, *Earth Planet. Sci. Lett.*, *173*(1–2), 53–60, doi:10.1016/S0012-821X(99)00215-0.

Huang, S., C.-T. A. Lee, and Q.-Z. Yin (2014), Missing lead and high $^{3}He/^{4}He$ in ancient sulfides associated with continental crust formation, *Sci. Rep.*, *4*, 5314, doi:10.1038/srep05314.

Kaneoka, I. (1983), Noble gas constraints on the layered structure of the mantle, *Rock Magn. Paleogeophys.*, *302*(5910), 698–700, doi:10.1038/302698a0.

Kurz, M. D., W. J. Jenkins, and S. R. Hart (1982), Helium isotopic systematics of oceanic islands and mantle heterogeneity, *Nature*, *297*(5861), 43–47, doi:10.1038/297043a0.

Kurz, M. D., W. J. Jenkins, S. R. Hart, and D. Clague (1983), Helium isotopic variations in volcanic rocks from Loihi seamount and the Island of Hawaii, *Earth Planet. Sci. Lett.*, *66*, 388–406, doi:10.1016/0012-821X(83)90154-1.

Kurz, M. D., M. O. Garcia, F. A. Frey, and P. A. O'Brien (1987), Temporal helium isotopic variations within Hawaiian volcanoes: Basalts from Mauna Loa and Haleakala, *Geochim. Cosmochim. Acta*, *51*, 2905–2914, doi:10.1016/0016-7037(87)90366-8.

Kurz, M. D., M. Moreira, J. Curtice, D. E. Lott III, J. J. Mahoney, and J. M. Sinton (2005), Correlated helium, neon, and melt production on the super-fast spreading East Pacific Rise near 17°S, *Earth Planet. Sci. Lett.*, *232*, 125–142.

Kurz, M. D., J. Curtice, D. Fornari, D. Geist, and M. Moreira (2009), Primitive neon from the center of the Galápagos hotspot, *Earth Planet. Sci. Lett.*, *286*(1–2), 23–34, doi:10.1016/j.epsl.2009.06.008.

Lee, C.-T. A., P. Luffi, E. J. Chin, R. Bouchet, R. Dasgupta, D. M. Morton, V. Le Roux, Q. Yin, and D. Jin (2012), Copper systematics in arc magmas and implications for crust-mantle differentiation, *Science*, *336*(6077), 64–68, doi:10.1126/science.1217313.

Le Saout, M., A. Deschamps, S. A. Soule, and P. Gente (2014), Segmentation and eruptive activity along the East Pacific Rise at 16°N, in relation with the nearby Mathematician hotspot, *Geochem. Geophys. Geosyst.*, *15*, 4380–4399, doi:10.1002/2014GC005560.

Macdonald, K. C., P. J. Fox, S. Miller, S. Carbotte, M. H. Edwards, M. Eisen, D. J. Fornari, L. Perram, R. Pockalny, and D. Scheirer (1992), The East Pacific Rise and its flanks 8–18 N: History of segmentation, propagation and spreading direction based on SeaMARC II and Sea Beam studies, *Mar. Geophys. Res.*, *14*(4), 299–344.

Mahoney, J., J. M. Sinton, M. D. Kurz, J. D. MacDougall, K. J. Spencer, and G. W. Lugmair (1994), Isotope and trace element characteristics of a super-fast spreading ridge: East Pacific Rise, 13–23°S, *Earth Planet. Sci. Lett.*, *121*, 173–193.

Meyzen, C. M., J. Blichert-Toft, J. N. Ludden, E. Humler, C. Mével, and F. Albarède (2007), Isotopic portrayal of the Earth's upper mantle flow field, *Nature*, *447*, 1069–1074.

Mittelstaedt, E., G. Ito, and J. van Hunen (2011), Repeat ridge jumps associated with plume-ridge interaction, melt transport, and ridge migration, *J. Geophys. Res.*, *116*, B01102, doi:10.1029/2010JB007504.

Moreira, M., and C. Allègre (2004), Helium isotopes on the Macdonald seamount (Austral chain): Constraints on the origin of the superswell, *C. R. Geosci.*, *336*(11), 983–990, doi:10.1016/j.crte.2004.04.006.

Moreira, M., and C. J. Allègre (2002), Rare gas systematics on Mid Atlantic Ridge (37°–40°), *Earth Planet. Sci. Lett.*, *198*, 401–416.

Moreira, M., J. Kunz, and C. Allègre (1998), Rare gas systematics in popping rock: Isotopic and elemental compositions in the upper mantle, *Science*, *279*(5354), 1178–1181, doi:10.1126/science.279.5354.1178.

Moreira, M., R. Doucelance, B. Dupré, M. Kurz, and C. J. Allègre (1999), Helium and lead isotope geochemistry in the Azores archipelago, *Earth Planet. Sci. Lett.*, *169*, 189–205.

Moreira, M., L. Dosso, and H. Ondréas (2008), Helium isotopes on the Pacific-Antarctic ridge (52.5°–41.5°S), *Geophys. Res. Lett.*, *35*, L10306, doi:10.1029/2008GL033286.

Moreira, M., J. Escartin, E. Gayer, C. Hamelin, A. Bezos, F. Guillon, and M. Cannat (2011), Rare gas systematics on Lucky Strike basalts (37°N, North Atlantic): Evidence for efficient homogenization in a long-lived magma chamber system?, *Geophys. Res. Lett.*, *38*, L08304, doi:10.1029/2011GL046794.

Moreira, M., A. Kanzari, and P. Madureira (2012), Helium and neon isotopes in São Miguel Island basalts, Azores Archipelago: New constraints on the "low ^{3}He" hotspot origin, *Chem. Geol.*, *322–323*, 91–98, doi:10.1016/j.chemgeo.2012.06.014.

Mougel, B., A. Agranier, C. Hemond, and P. Gente (2014), A highly unradiogenic lead isotopic signature revealed by volcanic rocks from the East Pacific Rise, *Nat. Commun.*, *5*, 4474, doi:10.1038/ncomms5474.

Parai, R., S. Mukhopadhyay, and J. C. Lassiter (2009), New constraints on the HIMU mantle from neon and helium isotopic compositions of basalts from the Cook-Austral Islands, *Earth Planet. Sci. Lett.*, *277*(1–2), 253–261, doi:10.1016/j.epsl.2008.10.014.

Porcelli, D., J. Stone, and R. Onions (1987), Enhanced ^{3}He/^{4}He ratios and cosmogenic helium in ultramafic xenoliths, *Chem. Geol.*, *64*, 25–33.

Scheirer, D. S., and K. C. Macdonald (1993), Variation in cross-sectional area of the axial ridge along the East Pacific Rise: Evidence for the magmatic budget of a fast spreading center, *J. Geophys. Res.*, *98*(B5), 7871–7885, doi:10.1029/93JB00015.

Scheirer, D. S., and K. C. Macdonald (1995), Near-axis seamounts on the flanks of the East Pacific Rise, 8°N to 17°N, *J. Geophys. Res.*, *100*(B2), 2239–2259, doi:10.1029/94JB02769.

Shah, A. K., and W. R. Buck (2006), The rise and fall of axial highs during ridge jumps, *J. Geophys. Res.*, *111*, B08101, doi:10.1029/2005JB003657.

Stuart, F. M., S. Lass-Evans, J. G. Fitton, and R. M. Ellam (2003), High ^{3}He/^{4}He ratios in picritic basalts from Baffin Island and the role of a mixed reservoir in mantle plumes, *Nature*, *424*, 57–59.

Todt, W., R. A. Cliff, A. Hanser, and A. W. Hofmann (1996), Reading the isotope code, in *Earth Processes*, edited by S. R. Hart and A. Basu, pp. 429–437, AGU, Washington, D. C.

Weiland, C. M., and K. C. Macdonald (1996), Geophysical study of the East Pacific Rise 15°N–17°N: An unusually robust segment, *J. Geophys. Res.*, *101*(B9), 20,257–20,273, doi:10.1029/96JB01756.

Zindler, A., and S. Hart (1986), Chemical geodynamics, *Annu. Rev. Earth Planet. Sci.*, *14*, 493–571, doi:10.1146/annurev.earth.14.1.493.